

# Pressure and temperature effects on the degree of symmetry and chirality of the molecular building blocks of low quartz

Dina Yogev-Einot and David Avnir\*

Institute of Chemistry and The Lise Meitner  
Minerva Center for Computational Quantum  
Chemistry, The Hebrew University of Jerusalem,  
Jerusalem 91904, Israel

Correspondence e-mail:  
david@chem.ch.huji.ac.il

We establish quantitative correlations between pressure and temperature (PT) changes, and the degree of symmetry and of chirality of the main molecular building blocks of low quartz that these PT changes induce. The distortion from ideal tetrahedral symmetry, from helicity (deviation from  $C_2$  symmetry), and the level of chirality are evaluated quantitatively using the continuous-symmetry and chirality-measures approach. These measures are global and reflect all changes in bond angles and bond lengths. The specific molecular building blocks analyzed are the  $\text{SiO}_4$  elementary building block (which is found to be chiral!), the  $\text{Si}(\text{OSi})_4$  unit, the second-shell  $\text{SiSi}_4$  tetrahedron [composed of the five Si atoms of  $\text{Si}(\text{OSi})_4$ ] and the four-tetrahedra helix fragment,  $-\text{O}(\text{SiO}_3)_4-$ . The temperature and pressure effects on symmetry and chirality were found to mirror each other in all building blocks. By employing this quantitative approach to symmetry and chirality we were able to combine the pressure effects and temperature effects into a unified picture. Furthermore, the global nature of the symmetry measure allows the comparison of the behavior of isostructural materials such as germania and quartz. For these crystals it has been shown that the symmetry/chirality behavior of germania at low pressures is a predictor for the behavior of these structural properties in quartz at higher pressures. Finally, given that the rigid  $\text{SiO}_4$  unit undergoes only minor structural changes, it has been a useful observation that the symmetry/chirality of the small  $\text{SiSi}_4$  tetrahedron is a very sensitive probe for the symmetry and chirality changes in quartz as a whole.

Received 26 January 2004

Accepted 16 February 2004

## 1. Background

*Motto: 'If you know a thing only qualitatively, you know it no more than vaguely. If you know it quantitatively – grasping some numerical measure that distinguishes it from an infinite number of other possibilities – you are beginning to know it deeply. You comprehend some of its beauty and you gain access to its power and the understanding it provides' (Sagan, 1997).*

### 1.1. The aim of this study

We are interested in the question of how changes in pressure and temperature (PT) affect the symmetry and chirality of the molecular building blocks of crystalline extended structures. We approach this question by treating symmetry and chirality as quantitative structural parameters, which change continuously. Our model material for this study is

quartz, SiO<sub>2</sub>, particularly low ( $\alpha$ )-quartz. This abundant chiral material has been subjected to intensive PT studies because of its many applications in optics and electromechanics (Heizing, 1947). An early example of a temperature–structure correlation study of quartz is given by Le Chatelier (1889). Quartz is particularly prone to PT structural effects because, while being one of the hardest materials in nature, it is at the same time also one of the most compressible minerals. The source of this compressibility is the flexibility of the link between adjacent SiO<sub>4</sub> tetrahedra that share a common oxygen: This link is ten times more compressible than the rigid SiO<sub>4</sub> unit (Hazen & Finger, 1985). This PT-induced compressibility can be expressed by two angles: the Si–O–Si bond angle and the tilt angle (Glinnemann *et al.*, 1992; defined as the angle of rotation around the twofold axis of the SiO<sub>4</sub> tetrahedron).<sup>1</sup> For example, the tilt angle in low quartz changes from 16.1 to 26.7° when the pressure is increased from atmospheric to 13.1 GPa (Kim-Zajojonz *et al.*, 1990); it also decreases from 16.1 to 0° by increasing the temperature from 298 K up to the temperature of the phase transition to high quartz (846 K; Heaney, 1994). The interesting and important observation that pressure and temperature have *opposing* effects (Glinnemann *et al.*, 1992; Grimm & Dorner, 1975; Hazen & Finger, 1984) on the molecular building blocks of quartz is illuminated in this report from symmetry and chirality perspectives.

Traditionally, PT-induced structural changes have been studied in relation to *specific* geometric parameters, such as bond lengths, angles and unit-cell dimensions (Glinnemann *et al.*, 1992; Grimm & Dorner, 1975; Jorgensen, 1978; Lager *et al.*, 1982). However, since PT changes affect practically *all* bonds and *all* angles and therefore also the unit-cell parameters, correlations with only one of these specific structural characteristics are bound to omit the overall effect on the structure as a whole. Indeed, Thompson *et al.* addressed this problem by introducing a parameter which quantifies distortion from the ideal closest-packing (Thompson & Downs, 2001; see also the review in the *Introduction* to that paper).

A structural feature which encompasses all of the changes in bonds and angles is the *symmetry and chirality* of the molecular building units. While it has been known on a qualitative level that PT affect not only specific geometric parameters, but also the symmetry (and the chirality) of the whole, quantification of this global parameter in a continuous way has only become available in recent years (Alvarez *et al.*, 2001). We recall that the standard approach to symmetry has been to use it in ‘jumps’ and not as a continuous property. Thus, in their pioneering study of temperature effects on quartz, Bragg & Gibbs (1925) found that the phase transition between low and high quartz is associated with an increase in the symmetry of the phase (from P<sub>3</sub><sub>1</sub>21 to P<sub>6</sub><sub>2</sub>22 or from P<sub>3</sub><sub>2</sub>21 to P<sub>6</sub><sub>4</sub>22; see also §3 for a comment on the context of Landau’s order parameter; Landau & Lifshitz, 1958); but the question of how symmetry changes *within* a phase as PT change – the topic of this report – remained unanswered.

<sup>1</sup> This rotation angle eventually leads to a phase transition from high to low quartz (Grimm & Dorner, 1975); in high quartz this angle is defined as zero.

In recent years we developed a detailed methodology and computational tools which quantify symmetry and chirality (described in the next section), and these have been applied to numerous useful applications in various domains of chemistry, biochemistry and physical chemistry (see Alemany *et al.*, 2003; Alvarez, 2003; Alvarez & Avnir, 2003; Alvarez *et al.*, 2002; Alvarez & Llunell, 2000; Asakawa *et al.*, 2002; Aullon *et al.*, 2002; Bellarosa & Zerbetto, 2003; Casanova *et al.*, 2003; Estrada & Avnir, 2003; Kane, 2002; Lipkowitz & Schefzick, 2002; Pinsky *et al.*, 2003, for some recent examples; see also our review in Avnir *et al.*, 1998). Using this quantitative approach to symmetry and chirality, the main questions we have asked were: First (as mentioned above), how do changes in PT affect the symmetry and the chirality of a material on a molecular level? Second, do predictive correlations between pressure or temperature and quantitative symmetry/chirality exist? Third, in the context of symmetry, can PT effects be unified into one picture?

## 1.2. Measurement of the degree of symmetry and chirality

We briefly review the elements of the methodology of measurement of symmetry and chirality needed for this report. The symmetry measurement tool is based on finding the minimal distances that the points (atom coordinates) of a shape (a molecule or a molecular fragment) have to undergo in order to attain the desired symmetry. According to the Continuous Symmetry Measure (CSM) methodology (Zabrodsky *et al.*, 1992, 1993), given a structure composed of  $N$  atoms, the coordinates of which are  $\{Q_k, k = 1, 2, \dots, N\}$ , one searches for the vertex coordinates,  $\{P_k, k = 1, 2, \dots, N\}$ , of the *nearest* perfectly  $G$ -symmetric (hypothetical) object. The only input then is the set of  $Q_k$  coordinates, their connectivity (optional) and the desired  $G$  symmetry. The search for  $P_k$  is a special distance-minimization problem in that the object to which the distance is computed is not known *a priori*, but searched. Several computational tools were developed towards this goal (Pinsky & Avnir, 1998; Zabrodsky & Avnir, 1995; Zabrodsky *et al.*, 1992, 1993) and once  $P_k, k = 1, 2, \dots, N$ , is found the symmetry measure is defined as

$$S(G) = 100 \times \min \frac{1}{N \times D^2} \sum_{k=1}^N |Q_k - P_k|^2$$

$$= 100 \times \min \frac{\sum_{k=1}^N |Q_k - P_k|^2}{\sum_{k=1}^N |Q_k - Q_0|^2}, \quad (1)$$

where  $Q_0$  is the coordinates vector of the center of mass of the investigated molecule and where the denominator is a mean-square size normalization factor,  $D$ , summing over all  $N$  distances from  $Q_0$  to the  $N$  atoms of that molecule. The bounds of the measure are from zero (*i.e.* the structure has the tested symmetry) to 1.  $S(G)$  reaches this maximal value for questions such as what is the degree of heptagonality of a pentagon (see Zabrodsky *et al.*, 1992, 1993, for an explanation). However, since such extreme questions are not common

in chemistry and often near-symmetries appear more interesting, the scale has been expanded for convenience to 100. All  $S(G)$  values, regardless of  $G$ , are on the same scale and therefore comparable: For instance, one can compare the degree of, say, being tetrahedral (the tetrahedrality,  $T_d$ -ness) and square planarity (the degree of  $D_{4h}$ -ness) of various distorted four-ligand molecules (Keinan & Avnir, 2001); one can compare  $S(C_2)$  with  $S(T_d)$  for the same molecule, or for different molecules, and so on.

Evaluating the chirality content,  $S_{\text{ch}}$ , of an object by the Continuous Chirality Measure (CCM) approach is an integral part of the CSM approach, since it is based on the determination of the distance to the nearest *achiral* symmetry point group, that is,  $S_{\text{ch}} = S(G_{\text{achiral}})$  (Zabrodsky & Avnir, 1995). A common situation is that the nearest achiral structure has (at least) one reflection plane and if this plane is the only symmetry element in the nearest asymmetric structure, then  $S_{\text{ch}} = S(C_s)$ . For instance, the nearest achiral structure to a helix may be a plane onto which the helix points have been collapsed (Katzenelson *et al.*, 2000). Again, chirality values and symmetry values are on the same scale (because it is the same tool), and thus the degree of chirality and the degree of, say,  $C_2$  can be compared either within the same molecule or between different molecules.

### 1.3. Molecular building blocks of quartz

We shall analyze PT effects on the symmetry and chirality of the following molecular building blocks of quartz (Fig. 1):

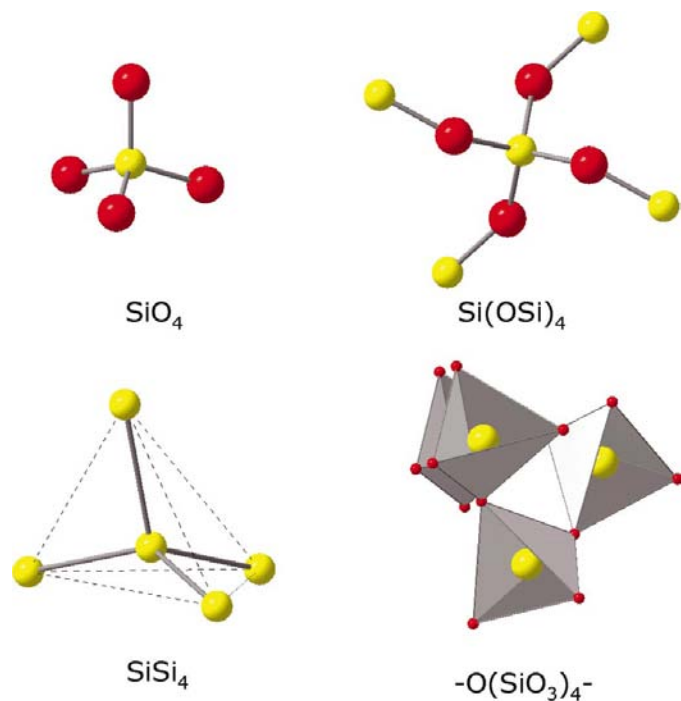


**Figure 1**  
The four building blocks of quartz crystal analyzed in this study: the first tetrahedron,  $\text{SiO}_4$  (top left); the  $\text{Si}(\text{OSi})_4$  unit (top right); the second tetrahedron,  $\text{SiSi}_4$  [bottom left, formed of the Si atoms of  $\text{Si}(\text{OSi})_4$ ]; the four  $\text{SiO}_4$  tetrahedra helix segment,  $-\text{O}(\text{SiO}_3)_4-$  (bottom right).

(i) The basic, slightly distorted  $\text{SiO}_4$  tetrahedron, which we term the first tetrahedron. The slight distortion from perfect tetrahedrality is such that *all* reflection mirrors are removed; *the  $\text{SiO}_4$  tetrahedron is therefore a chiral unit* (Yogev-Einot & Avnir, 2003).

(ii) The  $\text{Si}(\text{OSi})_4$  unit, which has a slightly distorted  $S_4$  achiral symmetry (improper axis of the order 4).

(iii) The  $\text{SiSi}_4$  tetrahedron within the  $\text{Si}(\text{OSi})_4$  unit, which we term the second-shell tetrahedron, and which is chiral as well.

(iv) The most characteristic molecular feature of quartz, namely the (chiral) helical laces of  $\text{SiO}_4$  tetrahedra, which determine its  $P3_221$  crystallographic chiral space group (with  $P3_121$  as its enantiomer). Of the various helical structures that can be identified within quartz (Glazer & Stadnicka, 1986), we selected for this study the one that stretches along the optical screw axis (the  $c$  axis of the unit cell). In practice we shall analyze a helical fragment of four tetrahedra,  $-\text{O}(\text{SiO}_3)_4-$ ,<sup>2</sup> because, as shown in Yogev-Einot & Avnir (2003), this fragment already carries all of the properties characteristic of the quartz helix and also because this fragment is the most chiral fragment (Yogev-Einot & Avnir, 2003).

Using (1) and several introductory  $S$  values from Yogev-Einot & Avnir (2003): For a specific quartz sample (Will *et al.*, 1988), under ambient conditions, the degree of tetrahedrality of the  $\text{SiO}_4$  unit (namely its distortion from  $T_d$  symmetry) and its degree of chirality were determined to be  $S(T_d) = 0.0094$  and  $S_{\text{ch}} = 0.0007$ , respectively. These are very small values, but nevertheless significant, as we shall see below. It is perhaps relevant to mention here that in several studies (*e.g.* in studies employing the RUM, Rigid Unit Mode approach; Tao & Sleight, 2003), this elementary building block has been assumed to be of perfect  $T_d$  symmetry and totally rigid. In the approach used here, this tetrahedron is not ideal and may be distorted.<sup>3</sup> The chirality of the compressible, nearly  $S_4$  unit of  $\text{Si}(\text{OSi})_4$  is indeed much higher:  $S(S_4) = S_{\text{ch}} = 0.74$ .<sup>4</sup> Likewise, the tetrahedrality distortion value of the  $\text{SiSi}_4$  sub-unit [which is derived from  $\text{Si}(\text{OSi})_4$ ] is much more pronounced [ $S(T_d) = 4.65$ ] compared with the small value found for the rigid  $\text{SiO}_4$  unit and so is its chirality value with  $S_{\text{ch}} = 0.56$ . In order to evaluate the degree of helicity of the helical fragment we use the most characteristic point-symmetry of a perfect helix, namely its  $C_2$  symmetry, where the  $C_2$  axis bisects the long helical axis. Perfect helicity is then characterized by  $S(C_2) = 0$ . Helices are of course chiral and so the second characteristic measure is  $S_{\text{ch}}$  of the helix. For the four-tetrahedra  $-\text{O}(\text{SiO}_3)_4-$  fragment we found  $S(C_2) = 1.25$  and  $S_{\text{ch}} = 16.23$  [which, as mentioned above, is  $S_{\text{ch}}(\text{max})$  for this material].

<sup>2</sup> In a previous report (Yogev-Einot & Avnir, 2003), we mistakenly denoted this fragment as  $(\text{SiO}_4)_4$ ; this should be corrected there to  $-\text{O}(\text{SiO}_3)_4-$ .

<sup>3</sup> Another important distinction between RUM and our approach is that RUM is a yes-or-no approach (*e.g.* Table 1 in Tao & Sleight, 2003), whereas we emphasize continuity.

<sup>4</sup> Since  $T_d$  is not a relevant symmetry for this unit,  $S(T_d)$  is not determined (although it can be calculated).

## 2. Pressure effects on the symmetry and chirality of quartz molecular building blocks

### 2.1. Observed correlations

We have collected the data from four different high-pressure X-ray studies of quartz (D'Amour *et al.*, 1979; Glinne-mann *et al.*, 1992; Hazen *et al.*, 1989; Jorgensen, 1978) and have searched for possible correlations between pressure and changes in the degree of chirality and symmetry of the various molecular building units listed above. From the largest unit [the helix segment,  $-\text{O}(\text{SiO}_3)_4-$ ] to the smallest one ( $\text{SiO}_4$ ), we first show in Fig. 2(a) a remarkable, nearly linear decrease in the degree of chirality of  $-\text{O}(\text{SiO}_3)_4-$  with pressure. This is, to the best of our knowledge, the first reported pressure/chirality correlation and one of a host of pressure/symmetry (*cf.* Alvarez, 2003) and other pressure/chirality correlations to be described. It is also noticeable that the chirality analysis of Fig. 2(a) successfully unifies all of the four different studies, which fall on the same line. Fig. 2(b) shows how the helicity of

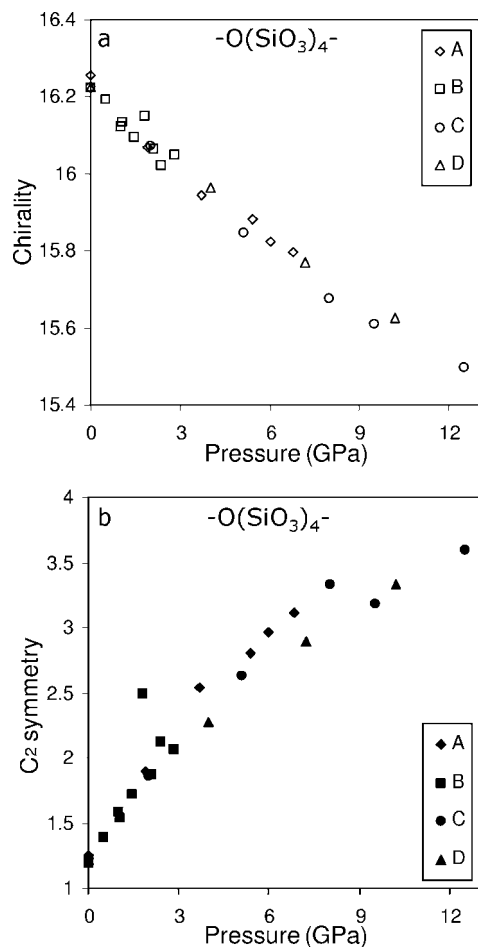


**Figure 2**  
The effect of pressure (a) on the degree of chirality and (b) on the helicity (the  $C_2$  symmetry content) of the helix fragment  $-\text{O}(\text{SiO}_3)_4-$  of low quartz. Data were taken from four different X-ray studies: A (D'Amour *et al.*, 1979), B (Jorgensen, 1978), C (Hazen *et al.*, 1989) and D (Glinne-mann *et al.*, 1992). (These data were also used in all the pressure figures. Also, in all these figures, 1 atm, which is 0.0001 GPa, is indicated as 0 on the GPa pressure scale).

this fragment, as determined through its  $C_2$  symmetry content, changes with pressure. Again, a clear symmetry–pressure correlation is observed, but this time in the opposite direction: The helicity becomes more distorted as the pressure increases.

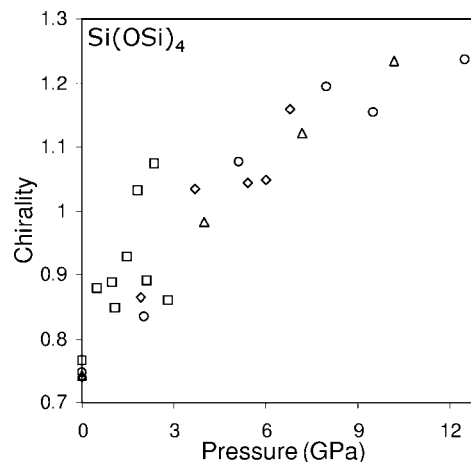


**Figure 3**  
The effect of pressure on the degree of chirality of the  $\text{Si}(\text{OSi})_4$  unit. See Fig. 2 for an explanation of the symbols.

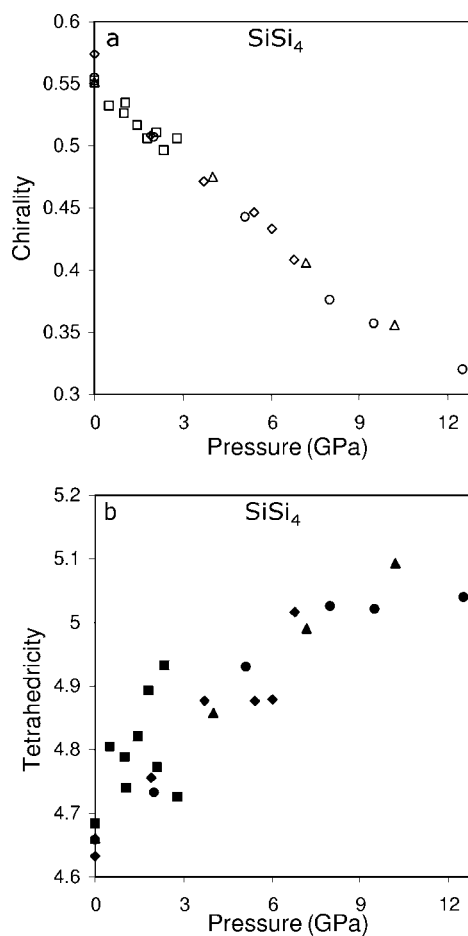


**Figure 4**  
The effect of pressure (a) on the degree of chirality and (b) on the degree of the tetrahedrality of the second tetrahedron,  $\text{SiSi}_4$ . See Fig. 2 for an explanation of the symbols.

**Table 1**  
Pressure effects on the symmetry and *chirality* of low quartz.

Symmetry deviation or chirality grows with pressure (+) and decreases with pressure (–).

Symmetry	SiO <sub>4</sub>	SiSi <sub>4</sub>	Si(OSi) <sub>4</sub>	–O(SiO <sub>3</sub> ) <sub>4</sub> –
$S(T_d)$	+	+		
$S_{ch}$	+	–	+	–
$S(C_2)$				+

Although helicity and chirality go hand-in-hand, the two opposite trends (Figs. 2*a* and *b*) are not contradictory: Helicity can be distorted in such a way that its chirality decreases. In general, in the following we shall encounter different and often opposite trends in the changes of the chirality and of the specific symmetries of the different units, but, as we shall see in §2.2, the different trends are compatible with each other and represent one picture.

Indeed, not only are there pressure/chirality and pressure/symmetry relations for the helix, but such correlations were also found for the smaller building blocks: Analysis of the compressible Si(OSi)<sub>4</sub> (Fig. 3) shows that its chirality increases with pressure (whereas, as just described, the chirality of the

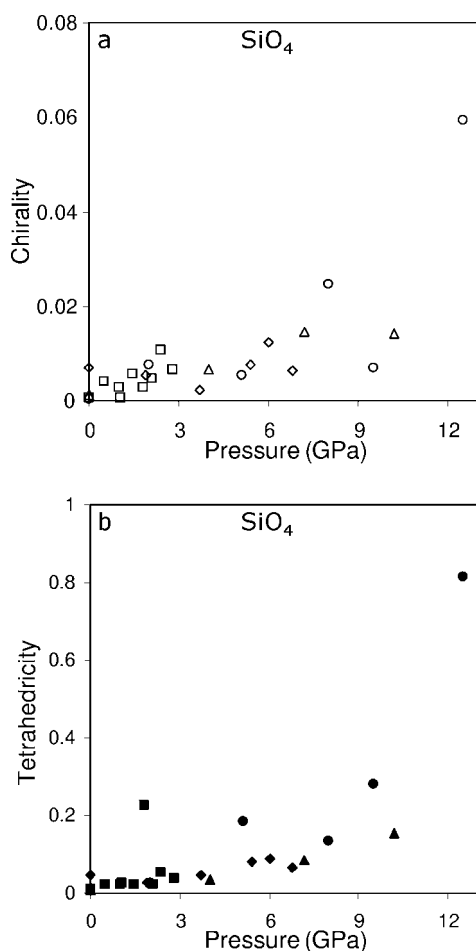


**Figure 5**  
The effect of pressure (*a*) on the degree of chirality and (*b*) on the degree of tetrahedrality of the smallest building block, the SiO<sub>4</sub> unit. See Fig. 2 for an explanation of the symbols.

helix was found to decrease with pressure; Fig. 2*a*). Next, being a sub-unit of Si(OSi)<sub>4</sub>, for the second-shell tetrahedron SiSi<sub>4</sub> one would perhaps expect to see a similar pressure/chirality trend, but again the trend reverses, as seen in Fig. 4*a*). For this unit one can also analyze the degree of tetrahedrality, and Fig. 4*b*) shows the correlation (more scattered) between the degree of tetrahedral distortion and pressure: The higher the pressure, the more distorted the tetrahedron.

Finally, we looked for a possible pressure effect on the symmetry of the most rigid unit, namely the basic SiO<sub>4</sub> tetrahedron. Indeed, as seen in Figs. 5*a*) and *b*), the pressure effects here are much smaller: *cf.* the chirality and symmetry values to those of the SiSi<sub>4</sub> unit (Figs. 4*a* and *b*; note the change in the chirality trend). Nevertheless, although the distortion is small, it is important to emphasize again that even the most elementary building unit of quartz is not perfectly tetrahedral and that the unit is chiral by itself.

Table 1 summarizes all the observed trends of the pressure effects. These trends are related because they all originate from the same specific distortions in angles and bond lengths that are due to the application of pressure. Yet we see that this distortion affects the various types of symmetries and the chirality of the specific building blocks in different, even opposing ways. Next we explain some representative trends in Table 1.

## 2.2. Analysis of the observed correlations

Let us begin by explaining why the chirality of the helix decreases with pressure. To do so it is helpful to shift our focus to the crystallographic unit cell: All three parameters decrease as pressure increases, but the changes are such that while length *a* remains equal to length *b*, the *ca* ratio increases (D'Amour *et al.*, 1979). The ratio increases because length *a* (and length *b*) decreases faster than length *c*. Since the helix is aligned along the *c* axis, this anisotropic change in unit-cell

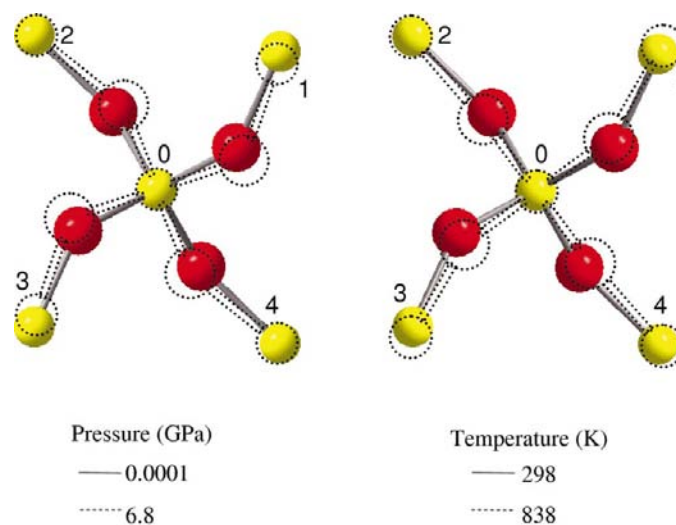


**Figure 6**  
The effects of pressure and temperature on the structure of Si(OSi)<sub>4</sub>. When pressure is increased (left) the Si1–Si3 distance (Si: yellow circles, O: red circles) contracts, while an increase in temperature causes that distance to expand.

parameters means that the radius of the helix decreases faster than its height. This thinning of the helix with pressure explains why its chirality decreases with pressure (Fig. 2a): The reader is directed to imagine the extreme case of a (close to) zero-radius helix, namely a line which is of course achiral. Interestingly, this change is associated with a distortion in the helicity [increase in the  $S(C_2)$  value, Fig. 2b]; *i.e.* the chiral helical unit is less of an ideal helix when pressurized. Since an ideal helix is already chiral, the distortion of helicity can go either way: Either a further increase in the chirality, or its decrease, depending on the specific anisotropic distortive

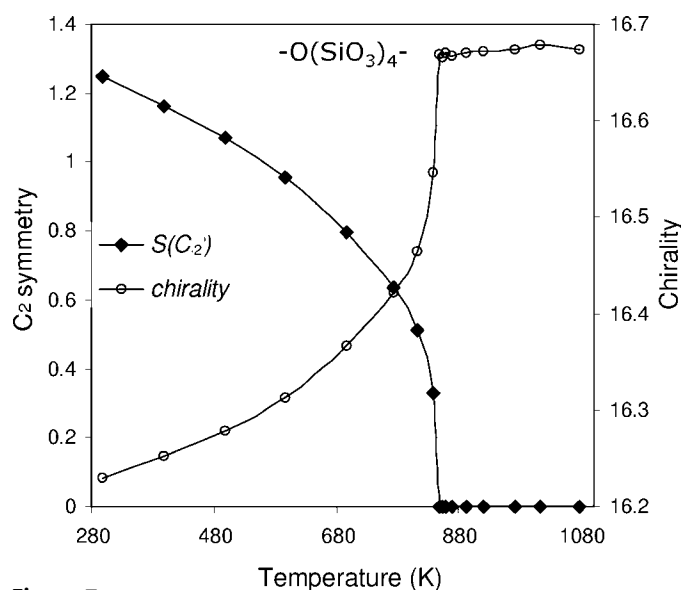


**Figure 7**  
Temperature effect on the degree of  $C_2$  symmetry and on the chirality of the helix fragment  $-\text{O}(\text{SiO}_3)_4-$ . The phase transition from low to high quartz is detected by the symmetry and chirality measures and is clearly seen at 848 K. Here and in the next figures the X-ray data are from Kihara (1990).

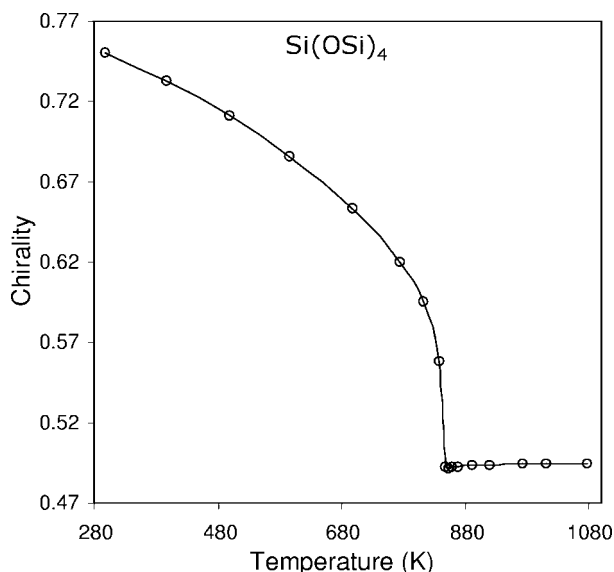


**Figure 8**  
Temperature effect on the degree of chirality of the  $\text{Si}(\text{OSi})_4$  unit. Again, the phase transition is clearly seen here and in Fig. 9.

modes of the units that build the helix. In our case this anisotropy (described next) distorts the  $C_2$  symmetry of the helix in the direction of achirality.<sup>5</sup> Moving on to the  $\text{Si}(\text{OSi})_4$  building block, the anisotropy induced by pressure is presented in Fig. 6 (left): Two of the Si atoms ( $\text{Si}1$  and  $\text{Si}3$ ) approach each other because of the reduction in the  $\text{Si}1-\text{Si}0-\text{Si}3$  angle from  $123.3$  to  $117.9^\circ$ ; at the same time, the other pair of Si atoms ( $\text{Si}2$ ) and  $\text{Si}4$ ) move farther apart because of the opening of the  $\text{Si}2-\text{Si}0-\text{Si}4$  angle from  $141.5$  to  $148.3^\circ$ . It should be noted that these different angle changes take place despite the fact that the four Si—O—Si bond angles undergo the same change, namely from  $142.2$  to  $132.4^\circ$ . Since the  $S_4$  operation [from which the  $\text{Si}(\text{OSi})_4$  building block slightly deviates] is composed of  $C_4$  rotation, followed by reflection, one can conclude that the departure from chirality with pressure is mainly due to the latter.

Continuing with the  $\text{SiSi}_4$  unit, we have seen that while pressure causes the tetrahedrality to distort (Table 1, Fig. 4), at the same time the achiral symmetry increases (*i.e.* the tetrahedron becomes less chiral). How can that be? To understand this let us examine what is the nearest achiral structure, as obtained from the chirality calculation (the  $\{P_k, k = 1, 2 \dots N\}$  set of coordinates). It turns out that this nearest structure is of  $C_{2v}$  symmetry and not  $T_d$ . Therefore, while  $S(T_d)$  measures the distance from perfect tetrahedrality, the chirality measure relies in this case on a different, less symmetric nearest reference shape, namely a tetra-coordinated species of  $C_{2v}$  symmetry. The specific pressure effect is therefore approaching  $C_{2v}$ , while deviating from  $T_d$ . From that point of view, a slight distortion of the  $\text{SiO}_4$  tetrahedron under pressure is simpler: As pressure increases, the tetrahedron becomes more distorted, leading to an increase in both  $S(T_d)$  and  $S_{\text{ch}}$ . This distortion is not surprising given that the  $\text{SiO}_4$  tetrahedron is nearly perfect to begin with.

### 3. Temperature effects on the symmetry and chirality of quartz molecular building blocks

Quartz crystals have been studied at many temperatures (Jay, 1933; Kihara, 1990; Lager *et al.*, 1982; LePage *et al.*, 1980; Wright & Lehmann, 1981). In general, the structural changes of low quartz caused by temperature changes were found to be smaller than the changes found in the pressure range described above. Thus, it was found that the unit-cell volume (to which we return in §4) only undergoes a 5% expansion by heating from 13 to 848 K, compared with an 18% volume contraction upon pressurizing up to 12.5 GPa (Glinemann *et al.*, 1992).

Here we chose to analyze, as a representative case, the data of Kihara (1990), who determined the structure of a low-quartz crystal at temperatures ranging from 298 to 1126 K from X-ray diffraction. Fig. 7 shows the temperature effect on the helical  $C_2$  symmetry and on the chirality of the

<sup>5</sup> Again, a hypothetical example of how this can happen: Imagine the above described thinning is to a plane (not to a line). In this case chirality decreases while  $C_2$  symmetry increases.

**Table 2**

Temperature effects on the symmetry and chirality of the molecular building blocks of low quartz.

Symmetry deviation or chirality grow with temperature (+) and decreases with temperature (–).

Symmetry	SiO <sub>4</sub>	SiSi <sub>4</sub>	Si(OSi) <sub>4</sub>	–O(SiO <sub>3</sub> ) <sub>4</sub> –
$S(T_d)$	–	–		
$S_{ch}$	?	+	–	+
$S(C_2)$				–

–O(SiO<sub>3</sub>)<sub>4</sub>– helical fragment (we comment on the evident phase transition below). The smaller structural effect of temperature compared with pressure is indeed reflected in the

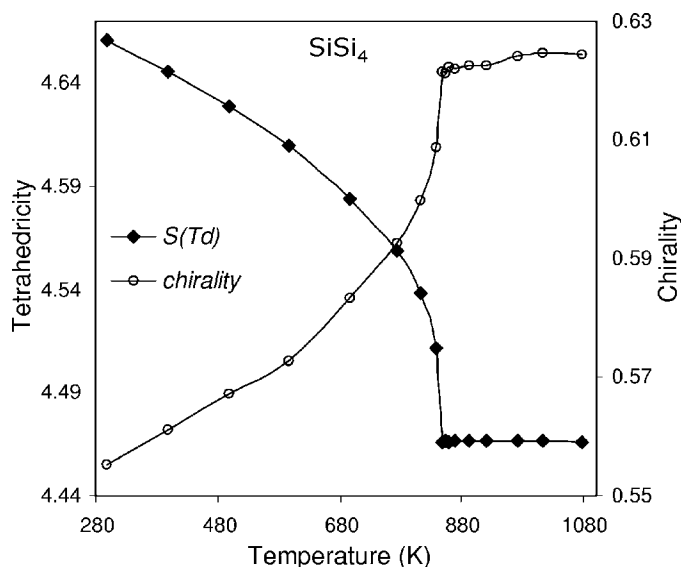


**Figure 9**  
Temperature effect on the degree of tetrahedrality of the SiSi<sub>4</sub> unit and on the degree of its chirality.

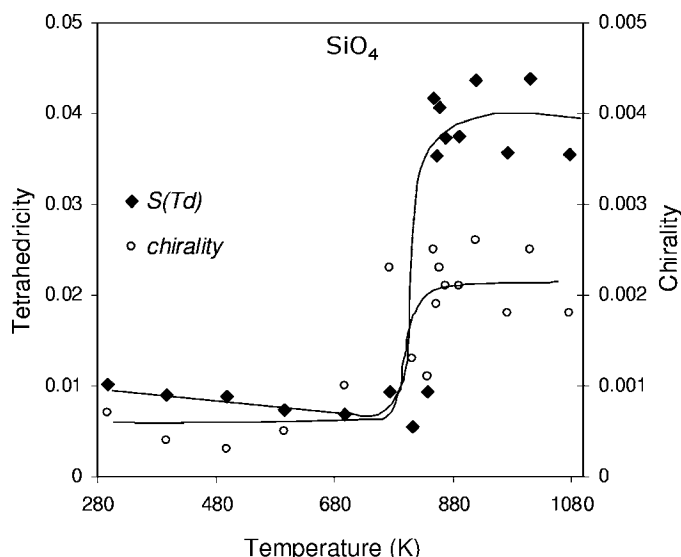


**Figure 10**  
Temperature effect on the degree of tetrahedrality and on the degree of chirality of the first tetrahedron, SiO<sub>4</sub>.

symmetry analysis: Compare the scales of Figs. 2 and 7. As in the case of pressure effects, here too the chirality and the symmetry measures change with opposite slopes (and are almost mirror images of each other). Figs. 8 and 9 show the temperature effects on the chirality and symmetry of the Si(OSi)<sub>4</sub> and SiSi<sub>4</sub> units. As for the rigid SiO<sub>4</sub>, it is seen in Fig. 10 that the small tetrahedral distortion decreases slightly with temperature and that the chirality changes are too small to reveal a trend.<sup>6</sup> All these trends are summarized in Table 2 and a very interesting feature is immediately seen: *Temperature and pressure effects mirror each other in all building blocks!*

The specific anisotropic atomic motions associated with an increase in temperature are shown in Fig. 6, where indeed the opposite directions of distortion, compared with the pressure-increase effect, are clearly seen. The atomic level explanations for the trends in Table 2 mirror those described for the pressure effects and therefore need not be repeated. Finally, this opposite trend is also true for the anisotropic change of the *c/a* ratio: Heating causes this ratio to decrease.

Although not the topic of this report, an important observation is that CSM and CCM detect very sensitively the phase transition to high quartz at 846 K (Figs. 7–10). Owing to the general importance of the phase transition phenomenon, we postpone its analysis in terms of the CSM and CCM methodologies to a subsequent report where we shall also relate these measures to the order parameter in the context of Landau’s theory (Dolino, 2000; Landau & Lifshitz, 1958). Briefly, the relationship to Landau’s approach is as follows: The order parameter, which has been used primarily for the analysis of phase transitions, may be of either physical or geometrical origin. The geometrical parameter, which is of relevance to our report, has been traditionally a *specific* geometrical parameter such as bond angle [for Landau treatment of quartz, see, for instance Dolino (2000)]. The symmetry measure in contrast is, as explained above, a *global-geometry* descriptor, that takes into account *all* the changes in bond lengths and bond angles. No such global order parameter has been included, to the best of our knowledge, within Landau’s formulation; work is in progress in this direction.

#### 4. Unification of the pressure and temperature effects

The fact that PT effects mirror each other (Tables 1 and 2) raises an interesting question: Can these effects on symmetry and chirality be unified into one picture, as was done with specific geometric parameters (Glinnemann *et al.*, 1992; Hazen & Finger, 1984)? One way to answer this question is to search for a secondary correlation between symmetry/chirality changes (which are due to both temperature and pressure effects) on the one hand, and on the other hand another parameter that is also affected by PT changes. One such parameter was already mentioned above, namely the PT behavior of the unit-cell *c/a* ratio (Glinnemann *et al.*, 1992).

<sup>6</sup> We recall here that the small distortion in SiO<sub>4</sub> was first noticed by Smith (1963), who based his conclusion on the analysis of the correlation between changes in the *c/a* ratio and changes in the Si–O distance with increasing temperature.

Indeed, such a PT-unifying correlation was found and is shown in Fig. 11: Here, the chirality of the  $-\text{O}(\text{SiO}_3)_4-$  helical fragment is plotted as a function of the  $c/a$  ratio for both

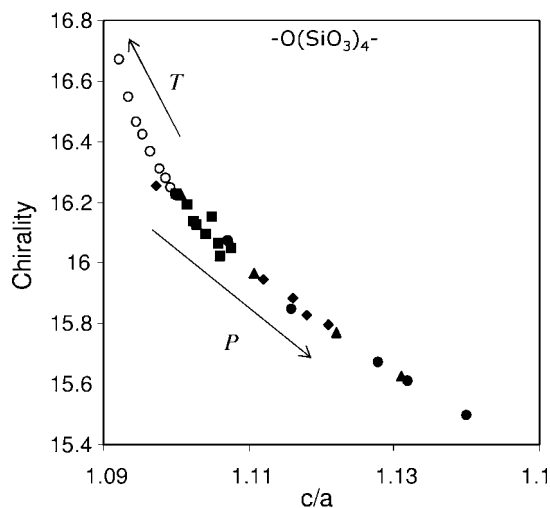


**Figure 11**  
The correlation between the degree of chirality of the helical fragment and the unit-cell  $c/a$  ratio, as a combined function of pressure (filled symbols) and temperature (open circles) changes.

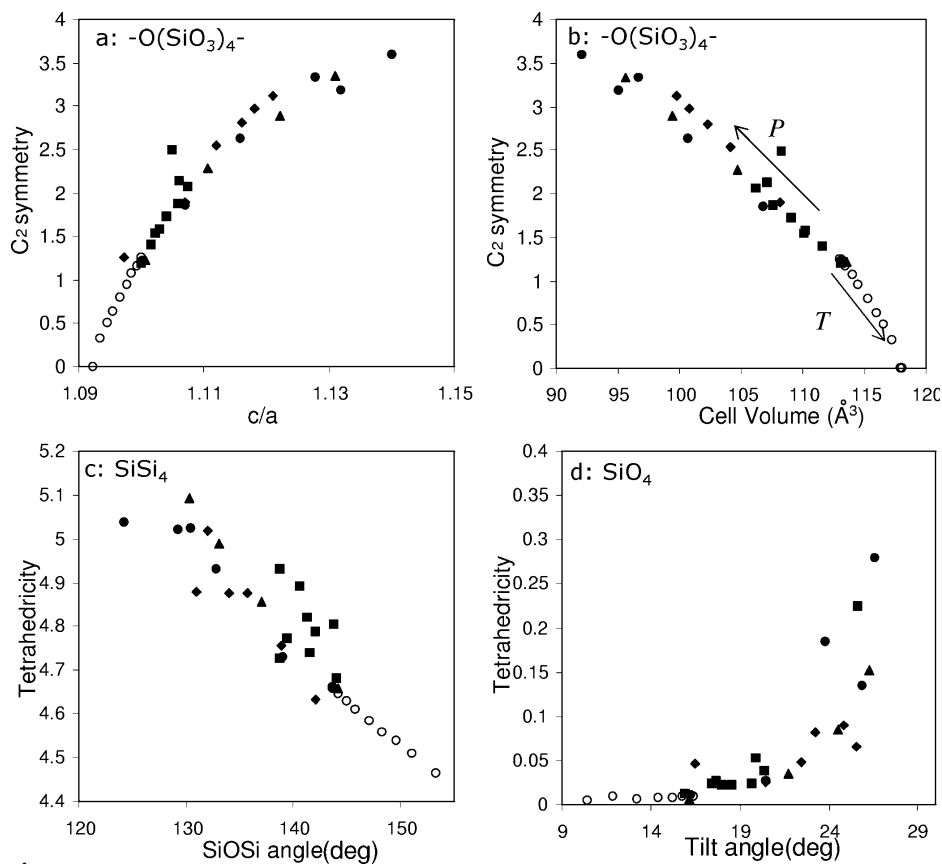


**Figure 12**  
Unified pressure (filled symbols) and temperature (open circles) effects on representative symmetry/structure correlations for various molecular units of low quartz. Correlations are shown between (a) the  $C_2$  symmetry of the helix fragment  $-\text{O}(\text{SiO}_3)_4-$  and the  $c/a$  ratio; (b) the  $C_2$  symmetry of the helix fragment  $-\text{O}(\text{SiO}_3)_4-$  and the cell volume; (c) the tetrahedrality of  $\text{SiSi}_4$  and the  $\text{Si}-\text{O}-\text{Si}$  angle; (d) the tetrahedrality of  $\text{SiO}_4$  and the tilt angle.

temperature changes (open circles) and pressure changes (filled symbols). It is seen that the temperature points and the pressure points form a single smooth curve. At the junction where the temperature points and pressure points meet (quite continuously), the temperature is  $\sim 300$  K and the pressure is  $\sim 1$  atmos. Then, from the junction and *up*, temperature increases and with it the chirality increases and  $c/a$  decreases; and, conversely, from that junction and *down*, pressure increases and with it chirality goes down and  $c/a$  increases. Figs. 12(a) and 13(a) show additional correlations of symmetry/chirality with  $c/a$ : The same continuity from high-pressure points to high-temperature points is repeated. (Owing to space limitations, not all the building blocks with their symmetries are shown, but the behavior is similar.)

Next, since the  $c/a$  ratio changes with PT, with  $a = b$ , it follows that the cell volume must also change (Glinnemann *et al.*, 1992) and hence PT/symmetry continuity should also be evident for this parameter. Indeed, Figs. 12(b) and 13(b) show this behavior for some typical symmetry–chirality/volume correlations. It also follows that since the unit-cell parameters reveal a unified PT/symmetry behavior, this should also be seen for specific molecular parameters. This prediction was tested for the inter-tetrahedral  $\text{Si}-\text{O}-\text{Si}$  angle and the tilt

angle defined above. Figs. 12(c), (d) and 13(c) and (d) show some representative results, which confirm this prediction. (Fig. 12(c) shows the most scattered data points we encountered; with regard to Fig. 12(d), note that the smooth PT transition is observed even for the slightly distorted first tetrahedron).

Thus, a consistent picture repeats itself for *all of the tested symmetries* (Figs. 11–13): Pressurizing and lowering the temperature work structurally in the same direction not only on specific bond lengths and angles (Hazen & Finger, 1984), but on the symmetry and chirality of the building blocks as a whole. Furthermore, the smoothness of the transition from pressure to temperature effects seems to indicate that the distortions under pressure changes and the distortions under temperature changes are of a similar nature (as was demonstrated in Fig. 6). It should be pointed out, however, that in this conclusion we differ from Glinnemann *et al.* (1992), who suggested different distortion mechanisms are induced by pressure and temperature. However, we do support the view of Hazen & Finger (1984), that inverse structural behavior is observed in low quartz, over



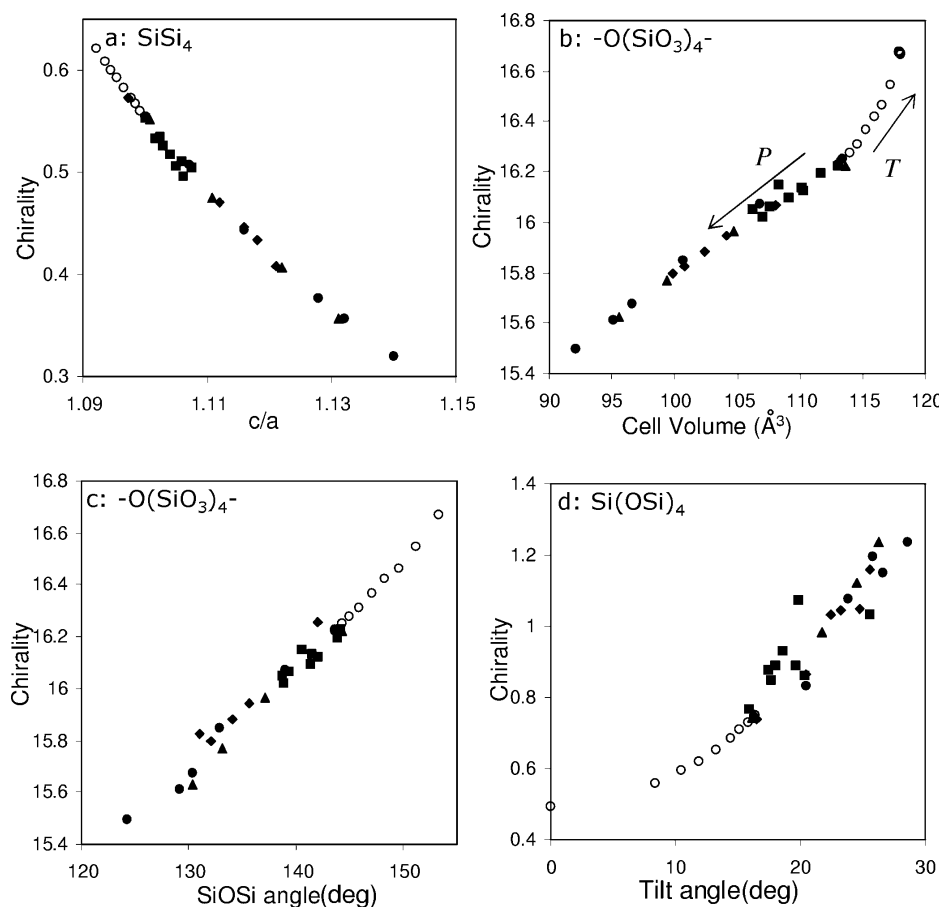


**Figure 13**

Unified pressure (filled symbols) and temperature (open circles) effects on representative chirality/structure correlations for various molecular units of low quartz. Correlations are shown between (a) the chirality of  $\text{SiSi}_4$  and the  $c/a$  ratio; (b) the chirality of the  $-\text{O}(\text{SiO}_3)_4^-$  unit and the cell volume; (c) the chirality of the  $-\text{O}(\text{SiO}_3)_4^-$  unit and the  $\text{Si}-\text{O}-\text{Si}$  angle; (d) the chirality of  $\text{Si}(\text{OSi})_4$  and the tilt angle.

the opposing view of Levien *et al.* (1980).

## 5. Quartz isostructural materials: germania

The global nature of the symmetry measure enables the comparison of symmetry and chirality properties of different crystals in general, and, in the context of this report, of oxides of different elements. As a specific example we shall now analyze low germania-quartz-type (germania or  $\text{GeO}_2$ , for short), which is isostructural with low quartz and which crystallizes in the same chiral, helical  $P3_221$  crystallographic space group. The studies of Jorgensen (1978) and Glinnemann *et al.* (1992) indicate that although the volume compression is almost identical for  $\text{SiO}_2$  and  $\text{GeO}_2$  (up to 10 GPa), the linear compressions along the  $a$  and  $c$  axes are different: Increasing pressure causes the  $c/a$  ratios for both materials to increase, but the magnitude of this increase for  $\text{GeO}_2$  is nearly twice that of  $\text{SiO}_2$  (see ref. Glinnemann *et al.*, 1992, for details). It is interesting then to see the similarities and the differences in the symmetry and chirality behavior of the building blocks of

these two crystals. As seen in Fig. 14, the response of germania to pressure shows the same trends and similar slopes as found for quartz: Fig. 14 shows six typical symmetry/chirality–pressure correlations [for the helical fragment  $-\text{O}(\text{GeO}_3)_4^-$ , for the second-shell tetrahedron  $\text{GeGe}_4$  and for the basic  $\text{GeO}_4$  unit], along with a comparison to the parallel units in low quartz. It is seen in Fig. 14 that while the germania symmetry data points (Figs. 14a, c and e) indicate a higher distortion compared with quartz (Figs. 14b and d), this distortion is such that the level of chirality diminishes for the larger units.  $\text{SiO}_4$  is, however, so rigid that  $\text{GeO}_4$  is more chiral, *i.e.* more distorted from achiral symmetry (Fig. 14f), reflecting the higher flexibility of the  $\text{GeO}_4$  tetrahedron to intra-tetrahedral distortion motions (Glinnemann *et al.*, 1992).

Chirality and symmetry analyses also provide a convincing confirmation of the proposition that the structural changes of germania at low pressures (Glinnemann *et al.*, 1992) (the pressures of Fig. 14) can serve as a good predictor of the structure of low quartz at high pressures (above 10 GPa; at this higher pressure range it is experimentally difficult to perform the X-ray diffraction experiment). The use of germania to predict the behavior of quartz is nicely

demonstrated in Fig. 15, where the pressure scale for quartz was extended artificially using the germania data points. Note that quartz at 10 GPa and germania at 1 atm (0.0001 GPa) are *isochiral* and *isosymmetric*, two concepts which indicate different structures which have the same chirality or symmetry values.<sup>7</sup>

## 6. Concluding remarks

This report has dealt with the quantitative analysis of the degree of symmetry and chirality of the building blocks of the quartz crystal and with their sensitivities to the external parameters, pressure and temperature (PT). We have shown, on a quantitative level, how PT changes affect these structural parameters, which are global in nature and combine within them all changes in bond lengths and angles. This approach has enabled us to unify pressure effects and temperature

<sup>7</sup> Owing to the size normalization and because the symmetry measure is a global parameter, isochirality and isosymmetry do not require the same size or the same specific geometry.

effects on symmetry and chirality into one picture, demonstrating the usefulness of this approach. Furthermore, the global nature of the symmetry measure allowed us to compare the properties of isostructural crystals such as germania and quartz.

An important conclusion emerging from our study is that small fragments of extended structures represent faithfully the behavior of the whole. Thus, given that the  $\text{SiO}_4$  tetrahedron undergoes only minor structural changes, it has been an interesting finding that the symmetry/chirality of the small  $\text{SiSi}_4$  tetrahedron is a very sensitive probe for the symmetry and chirality changes of quartz. This small building block has

the same symmetry/chirality behavior as the helix fragment and therefore contains all the information for the whole crystal.

In subsequent reports we shall address the relation between the optical properties of quartz and its chirality, and the description of the phase transition of quartz according to Landau's theory, in terms of changes in chirality and symmetry as order parameters.

*Program availability:* Scholars wishing to use the symmetry and chirality measurement programs are welcome to approach the authors.

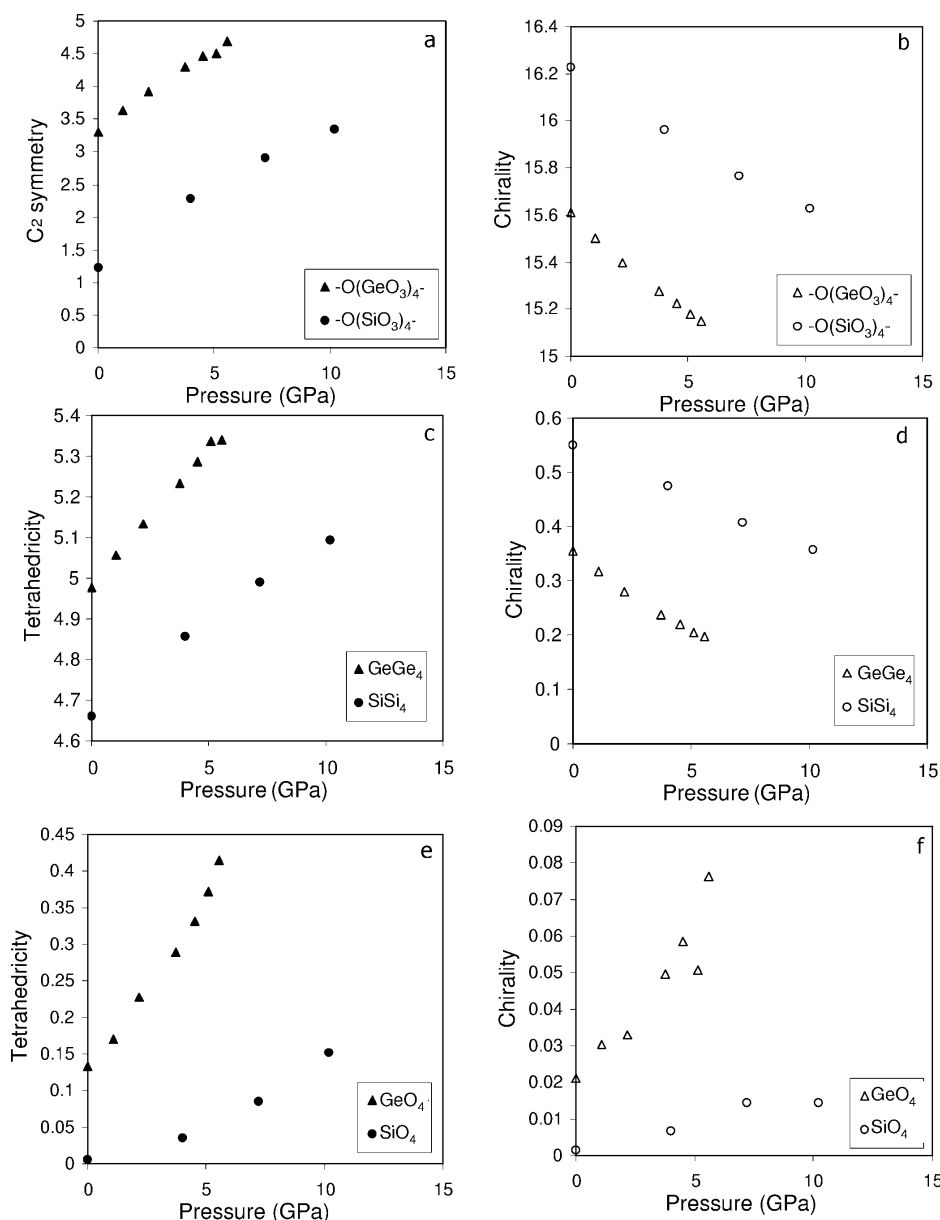


**Figure 14** Germania analysis: Pressure effects on (a) the helicity (the  $C_2$  symmetry content) of the  $-\text{O}(\text{GeO}_3)_4^-$  helical fragment; (b) the chirality of this fragment; (c) the degree of tetrahedrality of the second  $\text{GeGe}_4$  tetrahedron and (d) its chirality; (e) the degree of tetrahedral distortion and (f) the chirality of  $\text{GeO}_4$ . X-ray data from Glinnemann *et al.* (1992). Comparison with the equivalent units of  $\text{SiO}_2$  low quartz is provided as well (only for the data of *D* from Fig. 2).

Financial support of the Israel Science Foundation (Grant 30/01) is gratefully acknowledged. We thank Professor Kuniaki Kihara for helpful correspondence and for help in analyzing the crystallographic data of his work.

## References

Aleman, P., Alvarez, S. & Avnir, D. (2003). *Chem. Eur. J.* **9**, 1952–1957.  
 Alvarez, S. (2003). *J. Am. Chem. Soc.* **125**, 6795–6802.  
 Alvarez, S. & Avnir, D. (2003). *Dalton Trans.* pp. 562–569.  
 Alvarez, S., Avnir, D., Llunell, M. & Pinsky, M. (2002). *New J. Chem.* **26**, 996–1009.  
 Alvarez, S. & Llunell, M. (2000). *J. Chem. Soc. Dalton Trans.* pp. 3288–3303.  
 Alvarez, S., Pinsky, M., Llunell, M. & Avnir, D. (2001). *Cryst. Engng.* **4**, 179–200.  
 Asakawa, M., Brancato, G., Fanti, M., Leigh, D. A., Shimizu, T., Slawin, A. M. Z., Wong, J. K. Y., Zerbetto, F. & Zhang, S. (2002). *J. Am. Chem. Soc.* **124**, 2939–2950.  
 Aullon, G., Lledos, A. & Alvarez, S. (2002). *Angew. Chem. Int. Ed.* **41**, 1956–1959.  
 Avnir, D., Zabrodsky Hel-Or, H. & Mezey, P. G. (1998). *Encyclopedia of Computational Chemistry*, edited by P. von Rague Schleyer, pp. 2890. Chichester, UK: Wiley.  
 Bellarosa, L. & Zerbetto, F. (2003). *J. Am. Chem. Soc.* **125**, 1975–1979.  
 Bragg, W. H. & Gibbs, R. E. (1925). *Proc. R. Soc. London A*, **109**, 405–427.  
 Casanova, D., Boffill, J. M., Alemany, P. & Alvarez, S. (2003). *Chem. Eur. J.* **9**, 1281–1295.  
 D'Amour, H., Denner, W. & Schulz, H. (1979). *Acta Cryst.* **B35**, 550–555.  
 Dolino, G. (2000). *Structure and Imperfections in Amorphous and Crystalline Silicon Dioxide*, edited by R. A. B. Devine, J.-P. Duraud & E. Dooryhee, pp. 49–67. Chichester: Wiley.

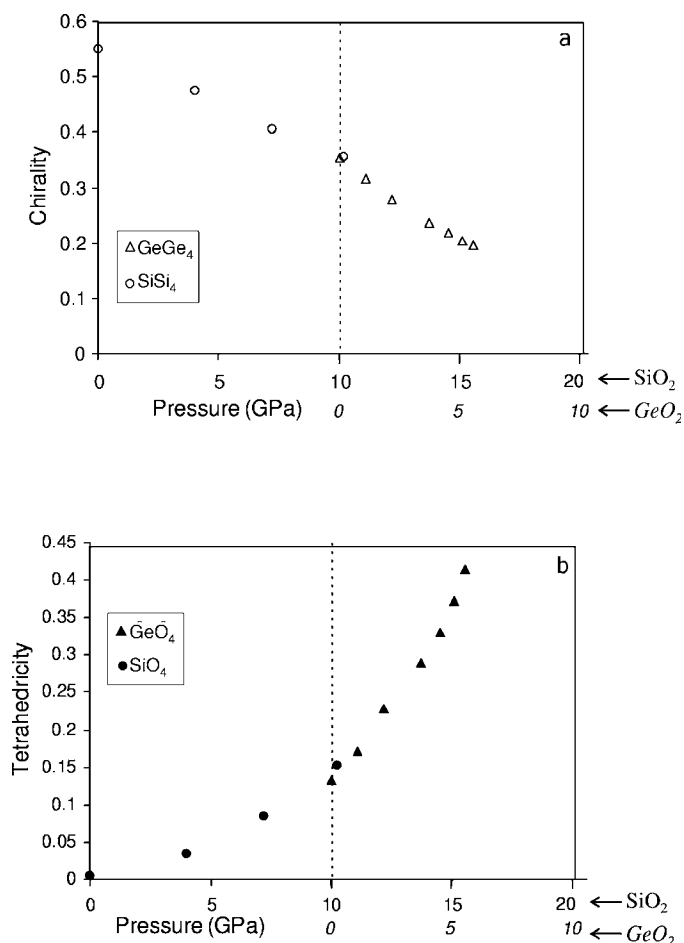


**Figure 15**  
 Indication that germania at low pressures is a predictor for the behavior of low quartz at higher pressures. The pressure scale for quartz is artificially extended, using the scale of germania. (a) The experimental data points for the chirality of SiSi<sub>4</sub> (circles) along with the predicted chirality values for that unit at higher pressures (triangles; these are also the GeGe<sub>4</sub> experimental points). (b) The experimental data points for the tetrahedrality of SiO<sub>4</sub> (circles) along with predicted values (triangles; these are also the GeO<sub>4</sub> experimental points) at higher pressures. Quartz at 10 GPa and germania at 1 atm (0.0001 GPa) are *isochiral* and *isosymmetric*.

Estrada, E. & Avnir, D. (2003). *J. Am. Chem. Soc.* **125**, 4368–4375.  
 Glazer, A. M. & Stadnicka, K. (1986). *J. Appl. Cryst.* **19**, 108–122.  
 Glinnemann, J., King Jr, H. E., Schulz, H., Hahn Th, LaPlaca, S. J. & Dacol, F. (1992). *Z. Kristallogr.* **198**, 177–212.  
 Grimm, H. & Dorner, B. (1975). *J. Phys. Chem. Solids*, **36**, 407–413.

Hazen, R. M. & Finger, L. W. (1984). *Comparative Crystal Chemistry*. Washington: Wiley.  
 Hazen, R. M. & Finger, L. W. (1985). *Science. Am.* **252**, 84–91.  
 Hazen, R. M., Finger, L. W., Hemley, R. J. & Mao, H. K. (1989). *Solid State Commun.* **72**, 507–511.  
 Heaney, P. J. (1994). *Silica, Physical Behavior, Geochemistry and Materials Applications*, edited by P. J. Heaney, C. T. Prewitt & G. V. Gibbs, pp. 1–39. Washington, DC: Mineralogical Society of America.  
 Heizing, R. A. (1947). *Quartz Crystals for Electrical Circuits*. New York: D. Van Nostrand Company, Inc.  
 Jay, A. H. (1933). *Proc. Phys. Soc. A*, **142**, 237–247.  
 Jorgensen, J. D. (1978). *J. Appl. Phys.* **49**, 5473–5478.  
 Kane, S. A. (2002). *Langmuir*, **18**, 9853–9858.  
 Katzenelson, O., Edelstein, J. & Avnir, D. (2000). *Tetrahedron: Asym.* **11**, 2695–2704.  
 Keinan, S. & Avnir, D. (2001). *Inorg. Chem.* **40**, 318–323.  
 Kihara, K. (1990). *Eur. J. Mineral.* **2**, 63–77.  
 Kim-Zajojonz, J., Werner, S. & Schulz, H. (1990). *Z. Kristallogr.* **214**, 324–330.  
 Lager, G. A., Jorgensen, J. D. & Rotella, F. J. (1982). *J. Appl. Phys.* **53**, 6751–6756.  
 Landau, L. D. & Lifshitz, E. M. (1958). *Statistical Physics*, pp. 424–445. Oxford: Pergamon Press.  
 Le Chatelier, H. (1889). *C. R. Acad. Sci.* **109**, 264.  
 LePage, Y., Calvert, L. D. & Gabe, E. J. (1980). *J. Phys. Chem. Solids*, **41**, 721–725.  
 Levien, L., Prewitt, C. T. & Weidner, D. J. (1980). *Am. Mineral.* **65**, 920–930.  
 Lipkowitz, K. B. & Scheffzick, S. (2002). *Chirality*, **14**, 677–682.  
 Pinsky, M. & Avnir, D. (1998). *Inorg. Chem.* **37**, 5575–5582.  
 Pinsky, M., Yogeve-Einot, D. & Avnir, D. (2003). *J. Comput. Chem.* **24**, 786–796.  
 Sagan, C. (1997). *Billions and Billions*, p. 21. New York: Random House.  
 Smith, G. S. (1963). *Acta Cryst.* **16**, 542–545.  
 Tao, J. Z. & Sleight, A. W. (2003). *J. Solid State Chem.* **173**, 442–448.  
 Thompson, R. M. & Downs, R. T. (2001). *Acta Cryst.* **B57**, 119–127.  
 Will, G., Bellotto, M., Parrish, W. & Hart, M. (1988). *J. Appl. Cryst.* **21**, 182–191.  
 Wright, A. F. & Lehmann, M. S. (1981). *J. Solid State Chem.* **36**, 371–380.  
 Yogeve-Einot, D. & Avnir, D. (2003). *Chem. Mater.* **15**, 464–472.  
 Zabrodsky, H. & Avnir, D. (1995). *J. Am. Chem. Soc.* **117**, 462–473.  
 Zabrodsky, H., Peleg, S. & Avnir, D. (1992). *J. Am. Chem. Soc.* **114**, 7843–7851.  
 Zabrodsky, H., Peleg, S. & Avnir, D. (1993). *J. Am. Chem. Soc.* **115**, 8278–8289.